AMERICAN SOCIETY FOR MICROBIOLOGY | mSphere®

RESEARCH ARTICLE

The Stickland Reaction Precursor *trans*-4-Hydroxy-L-Proline Differentially Impacts the Metabolism of *Clostridioides difficile* and Commensal *Clostridia*

A. D. Reed,[a] J. R. Fletcher,[a]* Y. Y. Huang,[c]* R. Thanissery,[a] A. J. Rivera,[a] R. J. Parsons,[a] A. K. Stewart,[b] D. J. Kountz,[c] A. Shen,[d] E. P. Balskus,[c] C. M. Theriot[a]

[a]Department of Population Health and Pathobiology, College of Veterinary Medicine, North Carolina State University, Raleigh, North Carolina, USA
[b]Molecular Education, Technology and Research Innovation Center, North Carolina State University, Raleigh, North Carolina, USA
[c]Department of Chemistry and Chemical Biology, Harvard University, Cambridge, Massachusetts, USA
[d]Department of Molecular Biology and Microbiology, Tufts University School of Medicine, Boston, Massachusetts, USA

A. D. Reed and J. R. Fletcher are co-first authors. Amber Reed and Joshua Fletcher contributed equally to this work. Author order was determined as Amber Reed was physically still present in the Theriot lab at the time of submission, while Joshua Fletcher had transitioned to a new position at the University of Minnesota.

ABSTRACT An intact gut microbiota confers colonization resistance against *Clostridioides difficile* through a variety of mechanisms, likely including competition for nutrients. Recently, proline was identified as an important environmental amino acid that *C. difficile* uses to support growth and cause significant disease. A posttranslationally modified form, trans-4-hydroxyproline, is highly abundant in collagen, which is degraded by host proteases in response to *C. difficile* toxin activity. The ability to dehydrate trans-4-hydroxyproline via the HypD glycyl radical enzyme is widespread among gut microbiota, including *C. difficile* and members of the commensal *Clostridia*, suggesting that this amino acid is an important nutrient in the host environment. Therefore, we constructed a *C. difficile* Δ*hypD* mutant and found that it was modestly impaired in fitness in a mouse model of infection, and was associated with an altered microbiota when compared to mice challenged with the wild-type strain. Changes in the microbiota between the two groups were largely driven by members of the *Lachnospiraceae* family and the *Clostridium* genus. We found that *C. difficile* and type strains of three commensal *Clostridia* had significant alterations to their metabolic gene expression in the presence of trans-4-hydroxyproline *in vitro*. The proline reductase (*prd*) genes were elevated in *C. difficile*, consistent with the hypothesis that trans-4-hydroxyproline is used by *C. difficile* to supply proline for energy metabolism. Similar transcripts were also elevated in some commensal *Clostridia* tested, although each strain responded differently. This suggests that the uptake and utilization of other nutrients by the commensal *Clostridia* may be affected by trans-4-hydroxyproline metabolism, highlighting how a common nutrient may be a signal to each organism to adapt to a unique niche. Further elucidation of the differences between them in the presence of hydroxyproline and other key nutrients will be important in determining their role in nutrient competition against *C. difficile*.

IMPORTANCE Proline is an essential environmental amino acid that *C. difficile* uses to support growth and cause significant disease. A posttranslationally modified form, hydroxyproline, is highly abundant in collagen, which is degraded by host proteases in response to *C. difficile* toxin activity. The ability to dehydrate hydroxyproline via the HypD glycyl radical enzyme is widespread among gut microbiota, including *C. difficile* and members of the commensal *Clostridia*, suggesting that this amino acid is an important nutrient in the host environment. We found that *C. difficile* and three commensal *Clostridia* strains had significant, but different, alterations to their metabolic gene expression in the presence of hydroxyproline *in vitro*. This suggests that the uptake and utilization of other nutrients by the commensal *Clostridia* may be

Editor Robert A. Britton, Baylor College of Medicine

Address correspondence to C. M. Theriot, cmtherio@ncsu.edu.

*Present address: J. R., Fletcher, Department of Microbiology and Immunology, University of Minnesota, 689 23rd Avenue SE, Minneapolis, MN 55455; Y. Y. Huang, Environmental Genomics and Systems Biology, Lawrence Berkeley National Laboratory, Berkeley, CA 94720.

The authors declare conflict of interest. CMT consults for Vedanta Biosciences, Inc. and Summit Therapeutics. CMT is a founder of CRISPR Biotechnologies.

Received 11 November 2021
Accepted 25 February 2022
Published 30 March 2022

affected by hydroxyproline metabolism, highlighting how a common nutrient may be a signal to each organism to adapt to a unique niche. Further elucidation of the differences between them in the presence of hydroxyproline and other key nutrients will be important to determining their role in nutrient competition against *C. difficile*.

KEYWORDS *Clostridioides difficile*, hydroxyproline, amino acids, *Clostridia*, Stickland reaction, colonization resistance, Stickland fermentation

Clostridioides difficile infection (CDI) is the cause of significant morbidity and mortality and is responsible for over 4.8 billion dollars in excess medical costs each year (1, 2). The current front-line treatment for CDI is the antibiotic vancomycin, which can resolve CDI (3). However, 20–30% of patients will experience a recurrence of CDI within 30 days, and 40–60% of the patients who have experienced one recurrence will have multiple recurrences (4, 5). The use of antibiotics, including vancomycin, is a major risk factor for CDI due to their effect on the gut microbiota, which causes a loss of colonization resistance against *C. difficile* (6–8). Colonization resistance, or the ability of the gut microbiota to defend against colonization by gastrointestinal pathogens such as *C. difficile*, has many potential mechanisms, including the production of inhibitory metabolites and competition for nutrient sources (9–11). Conversely, *C. difficile* toxin activity is associated with altered recovery of the gut microbiota, as well as liberation of numerous sugars and peptides/amino acids *in vivo* (12–15). However, it is unknown if *C. difficile* has a hierarchy of preferred nutrient sources in a host, or whether members of the microbiota also utilize similar nutrients, and if they do, whether their use contributes to colonization resistance.

Much of the research on colonization resistance against *C. difficile* has focused on the effects of secondary bile acids produced by the gut microbiota (16–20). While secondary bile acid metabolism is an important contributor, other factors such as competition for nutrients are also likely to play a role. For example, colonization of a host by nontoxigenic *C. difficile* can prevent colonization by toxigenic *C. difficile*, indicating that bacteria with similar nutritional needs can occupy an exclusive niche (21, 22). In addition, the increased amount of succinate available in the antibiotic treated gut promotes expansion by *C. difficile*, indicating that the depletion of the microbiota that occurs after antibiotic use creates a beneficial environment for *C. difficile* colonization and expansion (23). Metabolic and transcriptomic analysis have also shown that the availability of amino acids and other nutrients is very important in the early stage of CDI (15, 23, 24). Additionally, the degradation of collagen by host proteases that is induced by *C. difficile* toxin activity may be a source of peptides and amino acids to support *C. difficile* growth through the course of infection (14, 15).

C. difficile uses proline as an electron acceptor in Stickland metabolism for regeneration of NAD^+ and energy production, which involves ATP synthesis and generation of a proton motive force (25, 26). Given the importance of Stickland metabolism for *C. difficile*, it does not grow well in the absence of proline and other amino acids; therefore, it must compete for them within the host environment (27–29). The concentration of proline in media affects expression of genes in the *prd* operon, which encodes proline reductase and accessory proteins, with maximal expression observed when proline content is high (28). In addition, the availability of proline and branched chain amino acids in the gut correlates with increased susceptibility to *C. difficile* in a mouse model of infection (13). When a *C. difficile prdB* mutant that was unable to utilize proline as an energy source was tested in a mouse model of CDI, it was less fit *in vivo* and resulted in less toxin (TcdB) in stools when compared to mice challenged with wild-type *C difficile* (13). In addition, the presence of some commensal *Clostridia* causes an increase in the reliance of *C. difficile* on proline metabolism (30). This suggests that *C. difficile* may compete with some commensal *Clostridia* for proline in the gut. *C. difficile* also has a competitive advantage over the commensals *Clostridium scindens*, *Clostridium hylemonae*, and *Clostridium hiranonis* in a rich medium, although the extent to which this is due to the ability of *C. difficile* to utilize proline is unknown (16).

trans-4-Hydroxy-L-proline (hydroxyproline or Hyp) is a derivative of proline that has been posttranslationally modified by the host via prolyl-4-hydroxylase, and is a significant component of the highly abundant host protein collagen. Recently, we have shown that inflammation resulting from *C. difficile* toxin activity leads to increased expression of host matrix metalloproteinases and subsequent degradation of collagen, likely supplying *C. difficile* with hydroxyproline and other Stickland substrates (14). *C. difficile* can reduce hydroxyproline to proline in a two-step process that requires the glycyl radical enzyme 4-hydroxyproline dehydratase (HypD) and a pyrroline-5-carboxylate reductase (P5CR) encoded by the gene *proC* (30–32). Homologs of HypD are widespread in the gut microbiome, and a subset of organisms, largely *Clostridia*, that carry the *hypD* gene also encode an adjacent P5CR homolog, indicating that the ability of bacteria to reduce hydroxyproline may be useful in the gut (31). The widespread presence of HypD and the competitive fitness advantage gained by proline utilization indicates that it may play a significant role in *C. difficile* colonization in the gut (31, 33).

In this study, we hypothesized that use of hydroxyproline by *C. difficile* contributes to its fitness *in vivo*. We tested this by examining disease kinetics of wild-type (WT) *C. difficile* and a Δ*hypD* mutant in a mouse model of CDI. Mice challenged with the Δ*hypD* mutant had reduced weight loss, less toxin activity, and increased relative abundances of cecal *Lachnospiraceae*, a family which includes many commensal *Clostridia*, as well as members of the *Clostridium* genus. We also show that hydroxyproline affects the transcriptomes of *C. difficile* and three commensal *Clostridia* species (*C. scindens*, *C. hylemonae*, and *C. hiranonis*), though each had unique gene expression profiles, with alterations to pathways for carbohydrate and amino acid utilization among them. Together, these data show that *C. difficile* relies on hydroxyproline metabolism *in vivo* for robust sporulation and toxin production. Further, it identifies numerous metabolic pathways in *C. difficile* and commensal *Clostridia* that are affected by hydroxyproline, and the unique response of each organism indicates that hydroxyproline may act as a nutrient source and a signal to prime them for metabolism of other specific nutrients.

RESULTS

***C. difficile* requires *hypD* for maximum growth in a defined minimal media supplemented with hydroxyproline.** The reduction of hydroxyproline to L-proline is a two-step process requiring the *hypD* (*CD630_RS17450*) and *proC* (*CD630_RS17445*) genes (Fig. 1A) (32). To test the ability of *C. difficile* to utilize hydroxyproline, wild type, Δ*hypD*, Δ*proC*, and complemented strains were grown in a defined minimal medium (CDMM) with hydroxyproline substituted for proline at the same concentration (4.6 mM) (Fig. 1B). The Δ*hypD* mutant had a significant growth defect in the CDMM –Pro +Hyp, indicating that HypD is needed to utilize hydroxyproline ($p < 0.001$, Student's *t* test with Welch's correction). The Δ*proC* mutant had a modest growth defect in CDMM compared to the wild-type and Δ*hypD* strains, suggesting that P5CR may have multiple substrates or a larger role in amino acid metabolism in *C. difficile*. Unlike Δ*hypD*, the Δ*proC* mutant exhibited increased growth in CDMM –Pro +Hyp, indicating that P5CR is not essential for *C. difficile* to utilize hydroxyproline. The *C. difficile* 630Δ*erm* genome encodes a second *proC* homolog, *CD630_RS08190*, that may result in overlapping or functionally redundant roles with respect to hydroxyproline metabolism. Interestingly, the WT strain as well as Δ*proC* and both complements grew significantly better in CDMM –Pro +Hyp than they did in CDMM alone (<0.05, Student's *t* test with Welch's correction). As expected, all strains had very poor growth in CDMM –pro, as proline is essential for *C. difficile* growth.

The presence of *hypD* affects weight loss and toxin activity in a mouse model of CDI. To determine if hydroxyproline utilization is required for colonization and disease, WT C57BL/6J mice ($n = 8$ per group) were challenged with 10^5 spores of WT *C. difficile* or Δ*hypD*, and colonization and disease progression were measured for 7 days (Fig. 2A). There was no significant difference in vegetative *C. difficile* bacterial load in the feces during infection (Fig. 2B), but there was a significant decrease in fecal spores from Δ*hypD* challenged mice when compared to the WT challenge group on day 7 postchallenge (Fig. 2B and $p < 0.001$, Mann-Whitney). On day 7, bacterial enumeration

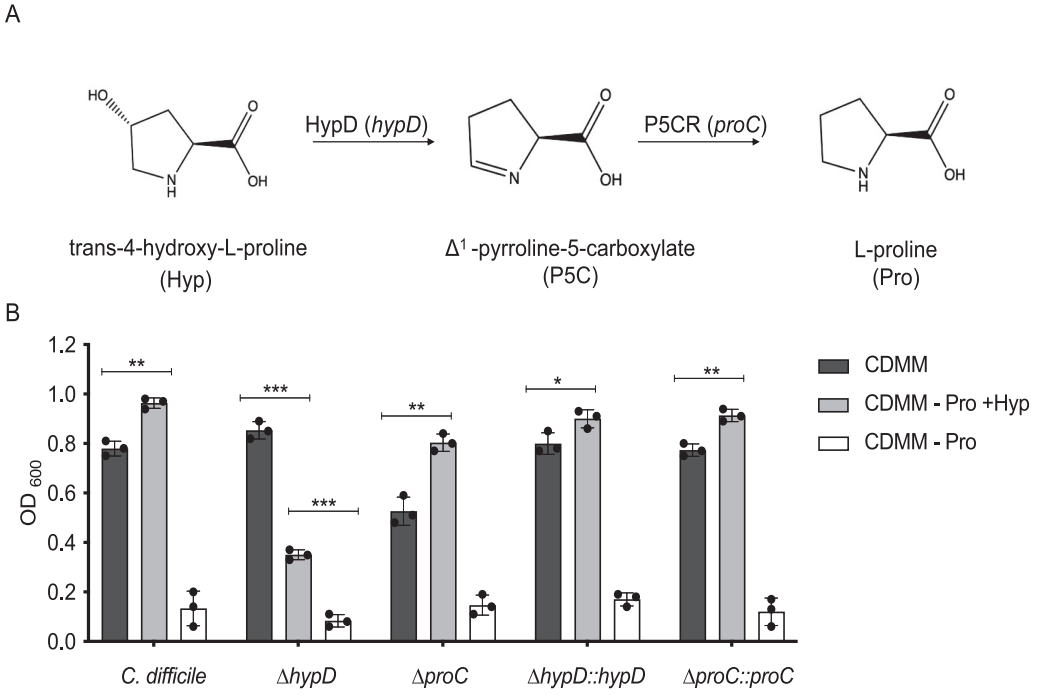

FIG 1 *C. difficile* Δ*hypD* mutant has a growth defect when hydroxyproline is substituted for proline in the growth medium. (A) Schematic depicting conversion of trans-4-hydroxy-L-proline to L-proline by HypD, gene *hypD* (*CD630_RS17450*), and P5CR, gene *proC* (*CD630_RS17445*). (B) Growth of *C. difficile* 630Δ*erm* WT, the Δ*hypD* and Δ*proC* mutants, as well as the complements of both mutants after 24 h of growth in the defined medium CDMM, in CDMM −proline +hydroxyproline (–Pro, +Hyp), and CDMM −proline (–Pro). Statistical significance was determined using Student's *t* test with Welch's correction to account for multiple comparisons (*, $P < 0.05$; **, $P < 0.01$; ***, $P < 0.001$; ****, $P < 0.0001$).

of cecal contents showed no significant difference in the level of *C. difficile* spores (Fig. S1A and B in the supplemental material), while the *C. difficile* vegetative cells were significantly higher in mice challenged with Δ*hypD* ($p < 0.05$, Mann-Whitney). The biggest difference between the groups was seen in the weights of the mice throughout CDI. WT challenged mice weighed significantly less than the cefoperazone control group (no *C. diff*) on days 3 ($p < 0.01$), 5 ($p < 0.001$), and 7 ($p < 0.05$) postchallenge (Fig. 2D, Kruskal-Wallis with Dunn's multiple comparisons). There was no significant difference in weights between the Δ*hypD* group and the no *C. diff* control group, indicating that the WT mice had increased clinical signs of disease compared to the Δ*hypD* group. This finding correlated with high toxin activity from the mice in the WT group compared to the Δ*hypD* group on Day 3 postchallenge (Fig. 2E and $p < 0.01$, Mann-Whitney), although the difference was not significant by Day 7.

Differences in the microbiota between mice challenged with WT *C. difficile* and Δ*hypD* are driven by members of the *Lachnospiraceae* family. To elucidate the reason behind the observed differences in CDI between mice challenged with WT and Δ*hypD*, the fecal microbiota of the no *C. diff*, WT, and Δ*hypD* mice were analyzed through V4 16S rRNA amplicon sequencing on day 0 as well as on days 2, 4, and 6 postchallenge (Data File S1). The cecal microbiota were analyzed on day 7 postchallenge, when necropsy occurred. When the alpha diversity was analyzed in the stool at the family level, there were significant differences between the no *C. diff* and Δ*hypD* groups on day 6, and when the cecal microbiota were analyzed on day 7, there were significant differences between all groups (Fig. S2A, Data File S2). When the beta diversity was analyzed using nonmetric multidimensional scaling analysis (NMDS), there were significant differences between the groups on days 2, 4, 6, and 7, indicating that there was a difference between the three groups after challenge with *C. difficile* (Fig. S2B). When only the infected groups were analyzed using NMDS, there were significant differences between the WT and Δ*hypD* groups on day 0 and day 7 (Fig. S2C). While the microbiomes did show differences on day 0 before *C. diff* challenge, all three

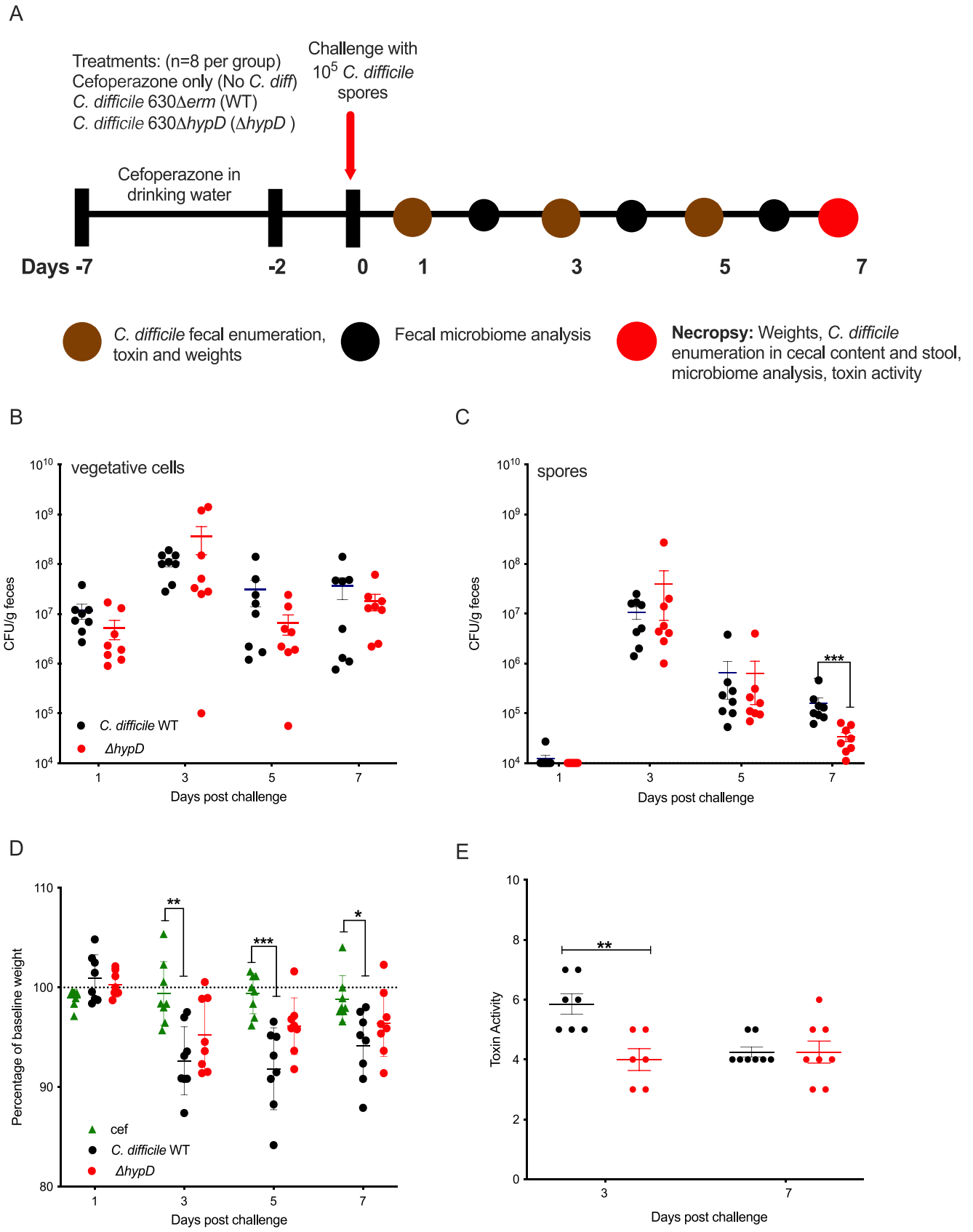

FIG 2 WT *C. difficile* induces more weight loss and toxin activity than the Δ*hypD* mutant in a mouse model of CDI. (A) Schematic depicting experimental design. All mice (n = 24) received the antibiotic cefoperazone in their drinking water. Subsets of mice were orally challenged with

(Continued on next page)

groups were dominated by *Enterococcaceae* (Fig. 3A). These differences are likely due to cage effects, but did not result in a significant difference when comparing the alpha and beta diversity of mice from day 0. Day 2 postchallenge had the highest relative abundance of *Peptostreptococcaceae*, the family to which *C. difficile* belongs, in both WT and Δ*hypD* mice, which was also when the greatest weight loss was observed (Fig. 1D). The amplicon sequence variant (ASV 6) classified as *Peptostreptococcaceae* resolved to *C. difficile*, so this was likely due to the expansion of *C. difficile* in the murine gut microbiota. By day 7 postchallenge, the *Lachnospiraceae* family made up a significant percentage of the cecal microbiota for all three groups, with the highest abundance being in the Δ*hypD* group at 73%, while the WT group and the no *C. diff* group had 60% and 43% abundance of *Lachnospiraceae*, respectively (Fig. 3A). Differential abundance analysis was calculated between the WT and Δ*hypD* groups using ALDEx2 (34). For each ASV analyzed, ALDEx2 estimates the difference in the centered-log-ratio (a measure of relative abundance) between groups and reports an effect size. The only day that had significant effect sizes for any ASVs was day 7, when the cecal microbiota were analyzed. Although only 3 ASVs were significant, the top 8 ASVs driving differences between the WT and Δ*hypD* microbiotas were examined via NCBI BLAST to determine the identity of each ASV (Fig. 3B, Data File S1). *Lachnospiraceae bacterium* strain D2 1 × 41 and *Clostridium* species MD294 were significantly higher in the WT microbiome than the Δ*hypD* microbiome. *Clostridium* species Clone 49 was significantly higher in the Δ*hypD* microbiota than the WT microbiota. There were also two *Lachnospiraceae* strains, including another ASV that resolved to *Lachnospiraceae bacterium* strain D2 1 × 41 as well as *Lachnospiraceae bacterium* DW17, that were higher in the Δ*hypD* microbiome, but did not reach significance. It is unclear why two separate ASVs that resolved to the same strain (*Lachnospiraceae bacterium* strain D2 1 × 41) showed such different results in terms of abundance in the WT and Δ*hypD* microbiotas, although it could be due to misassignment, as all 8 ASVs investigated via BLAST matched with multiple strains with high ID, and the highest match was selected to be the identified strain.

Of the top 8 ASVs driving the difference between the WT and Δ*hypD* cecal microbiomes on day 7 postchallenge, 5 were either *Clostridium* species or members of the *Lachnospiraceae* family, including all statistically significant ASVs (Fig. 3B). This suggests that hydroxyproline may be differentially abundant between the two groups of mice and that members of the *Lachnospiraceae* family and the *Clostridium* genus respond to this by utilizing it for growth. Given the previous work showing that commensal *Clostridia* are important to colonization resistance against *C. difficile*, we next wanted to investigate the response of commensal *Clostridia* to hydroxyproline (16, 19).

Hydroxyproline is utilized by commensal *Clostridia* and *C. difficile* when supplemented into a rich medium. To test for the utilization of hydroxyproline by *C. difficile* and the commensal *Clostridia* strains, WT *C. difficile*, Δ*hypD*, and the commensals *C. hiranonis*, *C. hylemonae*, and *C. scindens* were grown in BHI and in BHI + 600mg/L (4.6 mM) of hydroxyproline (BHI and BHI +Hyp) media for 14 h, then amino acids and 5-amino-valerate, the product of proline metabolism, were measured using LC/MS. As expected, the BHI +Hyp control had significantly higher levels of hydroxyproline than the BHI alone (Fig. 4A and $P < 0.01$, Student's *t* test with Welch's correction). WT *C. difficile* utilized hydroxyproline, as did all the commensal *Clostridia*; however, the Δ*hypD* mutant did not (Fig. 4A and $P < 0.01$, Student's *t* test with Welch's correction). There were no significant differences in levels of proline in bacterial cultures grown in BHI compared to BHI +Hyp, which is likely explained by the fact that the bacteria were

FIG 2 Legend (Continued)

C. difficile 630Δ*erm* (WT, $n = 8$) or *C. difficile* 630Δ*hypD*Δ*erm* (Δ*hypD*, $n = 8$). The third group of mice were only treated with cefoperazone (no *C. diff*, $n = 8$). (B–C) *C. difficile* vegetative cell (B) or spore (C) CFU in feces on days 1, 3, 5, and 7 postchallenge. (D) Mouse weights from 1, 3, 5, and 7 days postchallenge, shown as a percentage of baseline weight for each mouse from day 0. (E) Toxin activity on 3 and 7 days postchallenge. Statistical significance for data shown in B–E was determined using Mann-Whitney (*, $P < 0.05$; **, $P < 0.01$; ***, $P < 0.001$; ****, $P < 0.0001$).

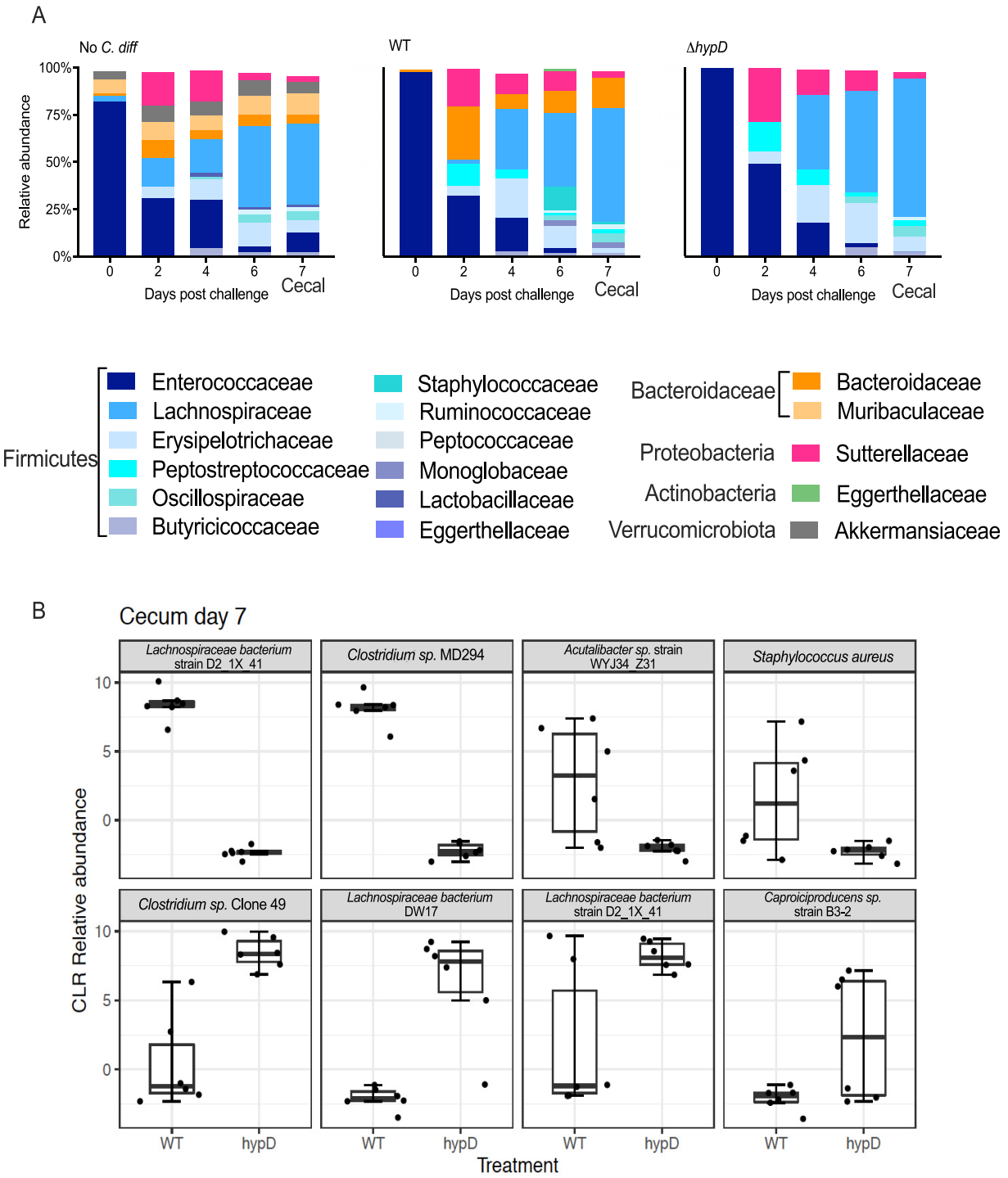

FIG 3 The *Lachnospiraceae* are important when determining the difference between the microbiota of mice challenged with WT and Δ*hypD*. (A) Relative abundance at the family level for no *C. diff*, *hypD*, and WT fecal microbiome for days 0, 2, 4, and 6 postchallenge and the cecal microbiome for day 7 postchallenge. (B) Top 8 ASVs driving differences between *hypD* and WT cecal microbiome on day 7 postchallenge. Significant ASVs ($q < 0.1$) are bolded.

grown in a rich medium and that proline is being metabolized into 5-amino-valerate and other intermediates (Fig. 4B). The levels of 5-amino-valerate were higher on average in supernatants for all bacteria grown in BHI or in BHI +Hyp than in the media control for either condition, indicating that all strains tested were likely utilizing proline and producing 5-amino-valerate (Fig. 4C, Data File S3). The levels of 5-amino-valerate

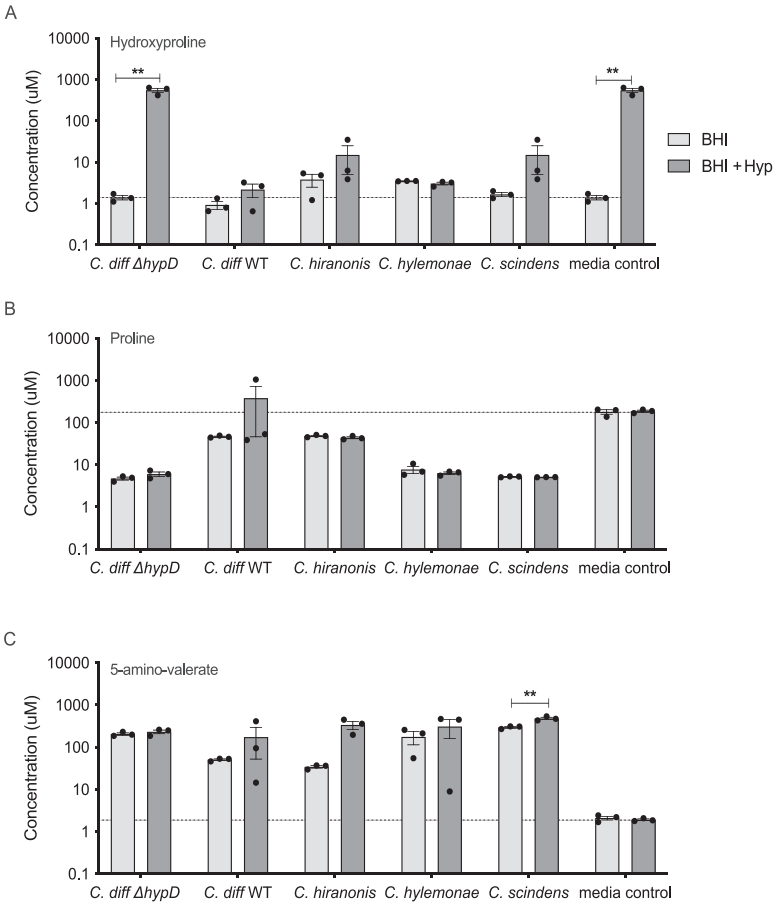

FIG 4 *C. difficile* WT, *C. hiranonis*, *C. hylemonae*, and *C. scindens* utilize hydroxyproline when it is supplemented into a rich growth medium. Concentration of (A) hydroxyproline, (B) proline, and (C) 5-amino-valerate in BHI and in BHI + 600 mg/L (4.6 mM) hydroxyproline. Supernatants were taken after 24 h of growth by WT, *hypD*, *C. hiranonis*, *C. hylemonae*, or *C. scindens*. BHI alone (dotted line) and BHI + 600mg/L (4.6 mM) of hydroxyproline were used as controls. Statistical significance was determined using Student's *t* test with Welch's correction to account for multiple comparisons (*, $P < 0.05$; **, $P < 0.01$; ***, $P < 0.001$; ****, $P < 0.0001$).

were significantly higher for *C. scindens* in BHI +Hyp, although it is unclear if the difference is biologically relevant ($P < 0.01$, Student's *t* test with Welch's correction).

The genomic position of *proC* in relation to *hypD* and the transcriptional response to hydroxyproline varies between *C. difficile* and commensal *Clostridia*. When *hypD* (CD630_RS17450) and *proC* (CD630_RS17445) were aligned across strains using *C. difficile* as the reference strain, it was found that only *C. difficile* and *C. hiranonis* had the *proC* gene next to the *hypD* gene (Fig. 5A). In *C. hylemonae* and *C. scindens*, the *proC* gene was not adjacent to the *hypD* gene. In addition, *hypD* from *C. hiranonis* showed the greatest amino acid identity (84%) to the *C. difficile* HypD protein while the other two commensals only showed 55% (Fig. 5A). All commensals showed a 69% AA identity to the P5CR protein encoded by *proC* in *C. difficile*. To determine if this would affect the transcriptional response of *hypD* and *proC* to hydroxyproline, *C. difficile*, *C. hiranonis*, *C. hylemonae*, and *C. scindens* were each grown in BHI or BHI +Hyp overnight, and the relative copy numbers of *hypD* and *proC* transcripts were analyzed using qRT-PCR (Fig. 5B to E).

All four strains tested had different transcriptional responses to hydroxyproline supplementation of rich media (Fig. 5B to E). *C. hiranonis* had significantly increased expression of *hypD* and *proC* in the presence of hydroxyproline, which was expected given that the two genes are possibly operonic in that strain ($P < 0.001$, Student's *t* test). *C. hylemonae* had significantly increased expression of *hypD*, but not of *proC* ($P < 0.01$, Student's *t* test). Neither *C. difficile* nor *C. scindens* showed significantly altered expression for either gene,

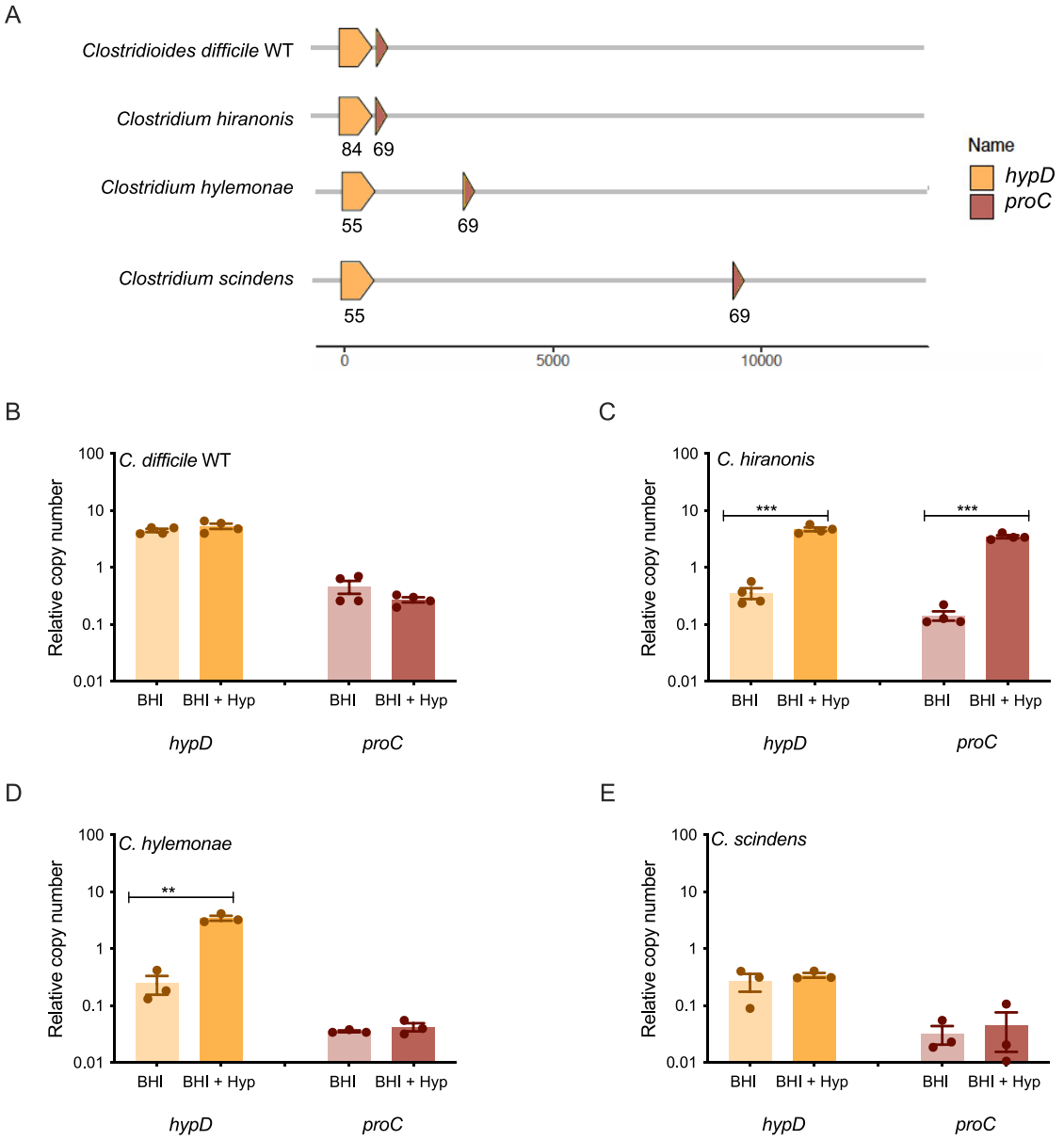

FIG 5 Expression of *hypD* and *proC* differs between *C. difficile* and selected commensal *Clostridia* in rich media supplemented with hydroxyproline. (A) Alignment of *hypD* and *proC* across *C. difficile* and selected commensal *Clostridia* strains. Each protein sequence was compared against its counterpart in the reference strain *C. difficile* 630Δ*erm*, generating the amino acid percent identity labeled within each gene. (B–E) Expression of *hypD* and *proC* in BHI media and BHI media with 600 mg/L (4.6 mM) hydroxyproline added of *C. difficile* (B), *C. hiranonis* (C), *C. hylemonae* (D), and *C. scindens* (E). Experiments were run in triplicate, and three biological replicates were performed. The expression in medium supplemented with hydroxyproline was compared to expression in medium without additional hydroxyproline. Statistical significance was determined using Student's *t* test (*, $P < 0.05$; **, $P < 0.01$; ***, $P < 0.001$; ****, $P < 0.0001$).

but the overall relative copy number for *C. difficile* was approximately 10-fold higher than the relative copy number for *C. scindens* (Fig. 5B and E).

***C. difficile* and commensal *Clostridia* each have different transcriptomic responses to the presence of hydroxyproline.** *C. difficile*, *C. hiranonis*, *C. hylemonae*, and *C. scindens* were all grown in BHI or BHI supplemented with 600 mg/L of hydroxyproline 4.6 mM (BHI +Hyp) media. At mid-log growth (OD_{600} 0.3–0.5), RNA was extracted, and the transcriptomic response was analyzed using RNAseq. For *C. difficile*, many of the genes that were upregulated upon exposure to hydroxyproline are involved in proline metabolism, including the copy of *proC* that is adjacent to *hypD*. In particular, many of the genes in the *prd* operon, which encodes enzymes for the reduction of proline and has previously

been shown to be upregulated in the presence of proline, were upregulated in *C. difficile* (Fig. 6A, Data File S4) (28). Genes involved in regenerating NAD+ via the reduction of succinate and its conversion to butyrate were decreased in expression in the presence of hydroxyproline, consistent with the role of proline reductase as a preferred mechanism of reducing equivalent regeneration. In *C. hiranonis*, most of the differentially expressed genes were downregulated, including amino acid and branched chain amino acid biosynthetic genes, as well as carbohydrate utilization genes. The putative ferrous iron importer gene *feoB2* was increased in *C. hiranonis* in the presence of hydroxyproline, as well as genes encoding a putative NADP-dependent α-hydroxysteroid dehydrogenase, although the overall expression of the latter was quite low (Fig. 6B). Similarly, *C. hylemonae* had several transcripts that significantly decreased with supplementation of hydroxyproline, including those encoding the glycine reductase (Fig. 6C). Conversely, the genes encoding the glycine cleavage system were increased in *C. hiranonis* in the presence of hydroxyproline. *C. scindens* had the largest number of differentially expressed genes between the two media conditions (Fig. 6D). A number of genes from the *prd* operon were upregulated in response to hydroxyproline, as were a number of genes encoding subunits of an electron transport complex (*rnfABCDGE*) (Fig. 6D). Several genes from the *bai* (bile acid inducible) operon were significantly decreased, although their expression levels in BHI alone were quite low. The expression of genes in the *bai* operon was decreased in *C. scindens* and *C. hylemonae*, in the presence of hydroxyproline, but in *C. hiranonis*, the expression of *bai* operon genes was increased in the presence of hydroxyproline (Fig. S3). Overall, the variable transcriptional responses to the presence of hydroxyproline observed between *C. difficile* and the three commensal *Clostridia* revealed changes in nonhydroxyproline associated metabolic pathways, including those for utilization of other Stickland substrates.

DISCUSSION

Understanding which nutrients are required for *C. difficile* to persist and cause disease in the host is important to developing targeted therapeutics against CDI. In this study, we employed bacterial genetics to examine how the utilization of hydroxyproline by *C. difficile* affects CDI and the microbiome in a mouse model of infection. To facilitate the interpretation of the *in vivo* data, the Δ*hypD* and Δ*proC* mutants and their complements were first grown in a minimal medium with hydroxyproline substituted for proline (CDMM –pro). While there was a growth defect in the Δ*hypD* mutant, as expected, no growth defect was observed for the Δ*proC* mutant (Fig. 1B). This is potentially due to functional redundancy within the *C. difficile* 630Δ*erm* genome, where a second homolog of P5CR is present (encoded by *CD630_RS08190*), which did not significantly change expression in the presence of hydroxyproline. Also of interest is that all strains other than the Δ*hypD* mutant showed significantly increased growth when hydroxyproline was present in the media as opposed to proline. This is likely due to the repression of alternative NAD^+ regeneration pathways that would result in butyrate production, which would impede growth of *C. difficile*, but further experiments are required to test this hypothesis (27, 31, 35).

Since Δ*hypD* growth was impaired *in vitro* when hydroxyproline was the only proline source, we reasoned that *hypD* may be important for colonization and disease progression in a mouse model of CDI. While the fecal burden of *C. difficile* was similar between the strains, the mice challenged with the WT strain showed more weight loss on days 3, 5, and 7 after challenge and toxin activity was higher on day 3 postchallenge relative to mice colonized with Δ*hypD* (Fig. 2D and E). There was no significant difference in toxin activity 7 days postchallenge, indicating that this effect is the strongest earlier during disease. While the effect is subtle, the differences in weight and toxin activity suggest that *C. difficile* may rely on hydroxyproline for maximal fitness *in vivo*, highlighting the importance of a host-derived amino acid that is likely made available via toxin-induced expression of host matrix metalloproteinases (14, 36, 37). As *C. difficile* is a nutritional generalist and the proline content of the murine gut is likely sufficient to support growth, removing the ability to utilize a single nutrient (hydroxyproline) via *hypD* mutation was not predicted to produce orders of magnitude

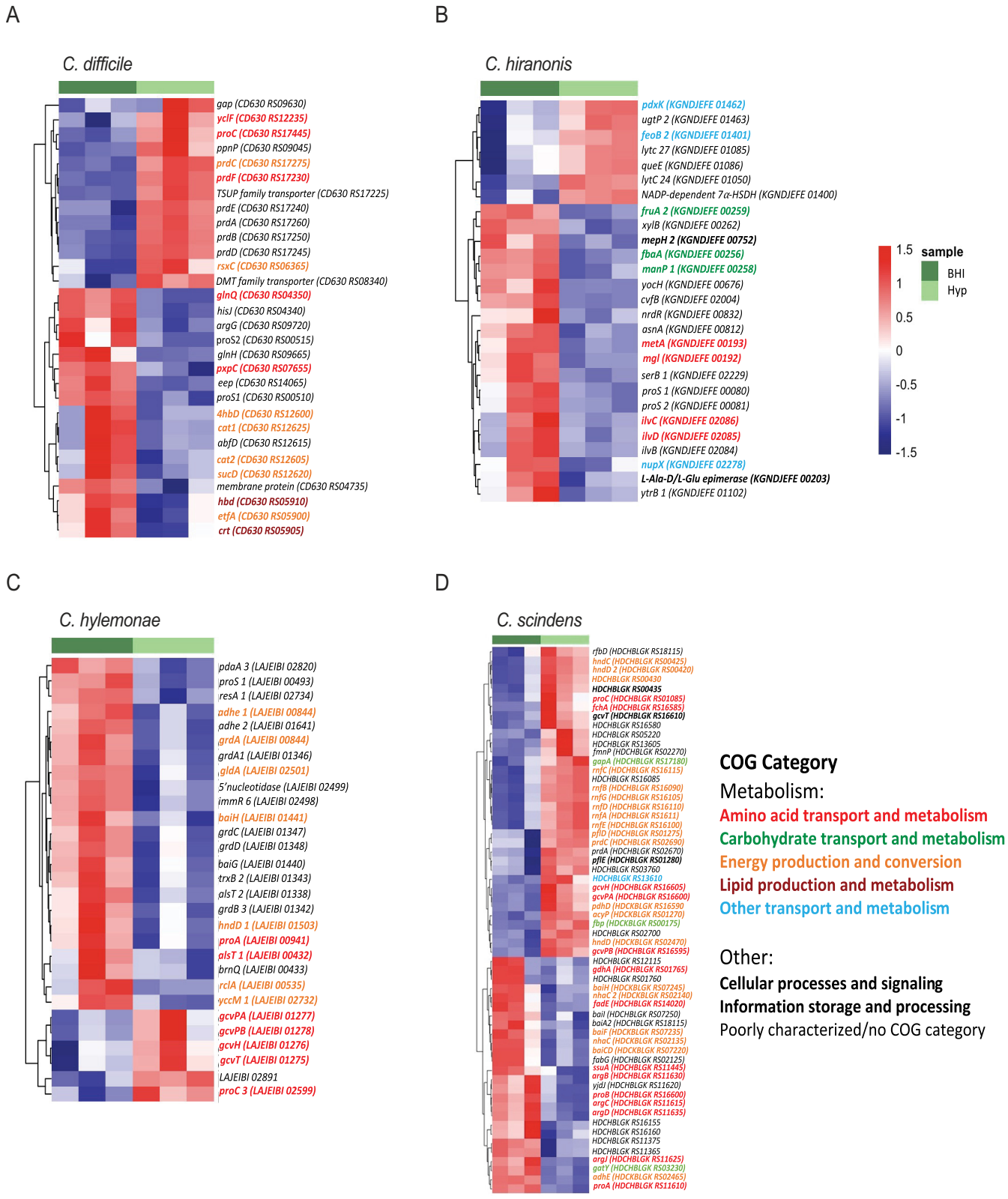

FIG 6 Transcriptomic differences in response to hydroxyproline vary between *C. difficile* and commensal *Clostridia*. Heatmap of genes that had significantly differential expression in (A) *C. difficile* WT, (B) *C. hiranonis*, (C) *C. hylemonae*, and (D) *C. scindens* between analyses was run using Geneious and DESeq2. All genes considered differentially expressed had an adjusted *P* value of <0.05 and ± 1 log fold change.

of difference in terms of colonization or disease. Rather, we hypothesized that the recovery of the microbiota over time after cefoperazone treatment and *C. difficile* challenge would allow for subtle phenotypes to emerge as newly colonizing bacteria would begin to utilize and possibly compete for hydroxyproline in the gut. Stochasticity in this process under the time scales studied here likely affects the magnitude of any such effects. *C. difficile* 630 was chosen for this experiment due to the genetic tools available for this strain, but it causes less severe disease in a mouse model than strains R20291 or VPI 10463 (38–40). It is possible that a stronger difference between the mutant and the wild-type strain would be observed in these strain backgrounds, especially given their increased expression of *hypD* in the presence of hydroxyproline in a defined medium when compared to *C. difficile* 630 (Fig. S4).

Each of the bacteria tested had a different transcriptional response to hydroxyproline, both in terms of RNAseq and when *hypD* and *proC* were tested individually using qRT-PCR (Fig. 5 and 6). Of particular interest was the fact that neither *C. difficile* nor *C. scindens* showed upregulation of *hypD* or *proC* when hydroxyproline was supplemented to the media, but when the levels of amino acids were quantified using LC/MS, both organisms metabolized the majority of hydroxyproline present (Fig. 4A). For *C. scindens*, this may mean that *hypD* and/or *proC* are always transcriptionally active or that the bacterium has another way to utilize hydroxyproline that does not require either gene. For *C. difficile* 630 Δ*erm*, it is more likely that *hypD* is always transcriptionally active, as *C. difficile* Δ*hypD* did not utilize the excess hydroxyproline added to the media, in addition to the growth defect previously observed (Fig. 1B and 4A). The lack of differential expression in *C. difficile* 630 is particularly interesting, as when the *C. difficile* strains 630, R20291, and VPI 10463 were tested in a minimal medium, 630 was the only one where *hypD* was not strongly upregulated in the presence of hydroxyproline, indicating that there are regulatory differences between strains (Fig. S4). Unfortunately, one of the limitations of the *in vitro* work in this study was the requirement to use a rich and undefined medium that contains a basal level of hydroxyproline, as *C. hiranonis* and *C. hylemonae* do not grow well in defined media (16, 41).

The overall transcriptional response of *C. difficile* 630Δ*erm* and the commensal *Clostridia* to hydroxyproline indicated *in vitro* that while there were some similarities, each organism had a relatively unique response. In *C. scindens*, over 60 transcripts were significantly altered in response to hydroxyproline, with 38 of those genes being in a metabolic COG category. Of particular interest is that *baiA2*, *baiCD*, *baiF*, *and baiH* were all downregulated in response to hydroxyproline, indicating that even without cholate in the media, the activation of the *bai* operon can vary depending on the nutritional content of the media. While none of the changes in *bai* transcripts in *C. hylemonae* were statistically significant, several *bai* operon genes, including *baiG* and *baiE*, were downregulated in response to hydroxyproline (Fig. S3). This is particularly interesting given the previous finding that *C. hylemonae* shows upregulation of the *bai* operon when exposed to cholate in a defined medium, but not when exposed to cholate in BHI (16, 41). Despite recent work that suggests bile acids do not play an essential role in protection against CDI, this study provides further evidence that there is a relationship between nutrient availability and secondary bile acid production in commensal *Clostridia* (42). Further work combining bile acids and hydroxyproline, and other amino acids important for Stickland metabolism, are needed to fully dissect transcriptional networks in these organisms and define their individual and combinatorial roles in colonization resistance against *C. difficile*. This supports the finding that each of these commensal *Clostridia* have differing metabolic responses to hydroxyproline, and that further elucidation of their nutrient utilization *in vivo* will be fruitful for identifying possible nutritional overlaps with *C. difficile*. This approach may allow for the development of rationally designed cocktails of commensal microbiota that can compete against *C. difficile* for one or more nutrient sources in an infected host.

MATERIALS AND METHODS

Animals and housing. C57BL/6J WT mice (5–8 weeks old; $n = 18$ male and $n = 18$ female) were purchased from Jackson Laboratory. The food, bedding, and water were autoclaved, and all cage changes were

performed in a laminar flow hood. The mice were subjected to a 12 h light and 12 h dark cycle. Mice were housed in a room with a temperature of 70°F and 35% humidity. Animal experiments were conducted in the Laboratory Animal Facilities located on the NCSU CVM campus. Animal studies were approved by NC State's Institutional Animal Care and Use Committee (IACUC). The animal facilities are equipped with a full-time animal care staff coordinated by the Laboratory Animal Resources (LAR) division at NCSU. The NCSU CVM is accredited by the Association for the Assessment and Accreditation of Laboratory Animal Care International (AAALAC). Trained animal handlers in the facility fed and assessed the status of animals several times per day. Those assessed as moribund were humanely euthanized by CO2 asphyxiation.

Mouse model of *C. difficile* infection. The mice were given 0.5 mg/mL cefoperazone in their drinking water for 5 days to make them susceptible to *C. difficile* infection, then plain water for 2 days, after which time they (n = 8, 4 males and 4 females) received 10^5 spores of either *C. difficile* 630Δ*erm* (WT) or *C. difficile* 630Δ*erm*Δ*hypD* (Δ*hypD*) via oral gavage. One group of mice (n = 8, 4 males and 4 females) received cefoperazone and no *C. difficile* spores (no *C. diff*) and were used as uninfected controls. Mice were weighed daily and monitored for clinical signs of distress (ruffled fur, hunched posture, slow ambulation, etc.). Fecal pellets were collected 1, 3, 5, and 7 days postchallenge and diluted 1:10 wt/vol in sterile PBS, then serially diluted in 96-well PCR plates and plated onto CCFA for enumeration of vegetative *C. difficile* CFU. The serially diluted samples were then removed from the anaerobic chamber and heated to 65°C for 20 min before being passed back into the chamber. The dilutions were plated onto TCCFA for enumeration of spore CFU. Additional fecal pellets were collected on days 1–7 and stored at −80°C for later use in toxin activity assays and 16S rRNA sequencing.

At day 7 postchallenge, mice were humanely sacrificed, and necropsy was performed. Cecal content was harvested for enumeration of vegetative *C. difficile* and spore CFU, as well as for toxin activity. Cecal tissue was harvested for 16S rRNA sequencing. Samples for sequencing and toxin activity were immediately flash frozen in liquid nitrogen and stored at −80°C until processing.

Toxin activity in the cecal content was quantified using the Vero Cell cytotoxicity assay (43). Briefly, the content was diluted 1:10 wt/vol in sterile PBS, and 10-fold dilutions were added to Vero cells in a 96-well dish for ~16 h. The reciprocal of the lowest dilution in which ~80% of the cells have rounded was reported as the titer.

Bacterial strain collection and growth conditions. The *C. difficile* strains used in this study were the wild type *C. difficile* 630Δ*erm* (WT) and the mutants *C. difficile* 630Δ*erm*Δ*hypD* (Δ*hypD*), *C. difficile* 630Δ*erm*Δ*proC* (Δ*proC*), *C. difficile* 630Δ*erm*Δ*hypD::hypD* (*hypD* complement), and *C. difficile* 630Δ*erm*Δ*proC::proC* (*proC* complement). All assays using *C. difficile* were started from spore stocks, which were prepared and tested for purity as described previously (43, 44). *C. difficile* spores were maintained on brain heart infusion (BHI) medium supplemented with 100 mg/L L-cysteine and 0.1% taurocholate (T4009, Sigma-Aldrich). Then cultures were started by inoculating a single colony from the plate into BHI liquid medium supplemented with 100 mg/L L-cysteine. The other bacterial strains used in this study were *C. hiranonis* TO 931, *C. hylemonae* TN 271, and *C. scindens* VPI 12708. All strains were maintained on 15% glycerol stocks stored in −80°C until use and were grown in BHI medium supplemented with 100 mg/L L-cysteine. All strains used in this study were grown under 2.5% hydrogen under anaerobic conditions (Coy, USA) at 37°C.

Growth studies in CDMM. *C. difficile* was grown in a well-established, defined minimal medium (CDMM) (28). CDMM –Pro +Hyp had 600 mg/L (4.6 mM) of *trans*-4-hydroxy-L-proline (Sigma) instead of L-proline. CDMM –Pro was used as a negative control. A single colony was inoculated into 5 mL of media and incubated at 37°C for 24 h, at which point the OD_{600} was measured using a spectrophotometer.

Construction of *C. difficile* strains. To construct the pMTL-YN1C-*hypD* complementation construct, primer pair YH-P295 and YH-P296 was used to amplify the *hypD* gene (Table S1). The resulting PCR product was digested with NotI and XhoI and ligated to pMTL-YN1C digested with the same enzymes. The resulting PCR fragments were inserted into pMTL-YN1C digested with NotI and XhoI using Gibson assembly (45). The assembly mixture was transformed into *E. coli* DH5α, and the resulting plasmids were confirmed by sequencing and then transformed into *E. coli* HB101/pRK24.

Vectors for gene deletion and complementation. To construct the pMTL-YN3-Δ*hypD* allelic exchange construct vector, ~1 kb flanking regions of *hypD* (CD630_RS17450) were PCR amplified from *C. difficile* 630 (primers listed in Table S1). To construct the pMTL-YN3-ΔproC allelic exchange construct, ~1kb flanking regions of *proC* (CD630_RS17445) were amplified. All PCRs were carried out using Phusion-HF Master Mix (NEB). PCR products were gel-purified using illustra GFX PCR DNA and Gel Band purification kit (GE Healthcare). Thirty ng of each flanking region of the targeted gene were used as templates for overlap PCR in 10 μL reactions (Ta of 72°C, extension time of 120s). Seven μL of each overlap PCR mix was used as template in 20 μL extension PCRs (Ta of 61°C, extension time of 60 sec) with flanking primers to amplify joined regions. The PCR SOE products were gel-purified and digested with AscI and SbfI. Each deletion template was ligated into AscI and SbfI-HF-linearized pMTL-YN3 using T4 DNA ligase (NEB) in 10 μL reactions at a 1:9 volume ratio (vector:insert). Ligation reactions were electroporated into *E. coli* TOP10 cells and plated out onto LB-chloramphenicol (25 μg/mL) agar plates.

To construct the pMTL-YN1C-*hypD* complementation construct, the promoter region, ~300 bp upstream of the HypD activase gene (CD630_RS17455), and *hypD* were separately amplified (Table S1). To construct the pMTL-YN1C-*proC* complementation construct, *proC* along with ~200 bp of the upstream region were amplified (Table S1). The resulting PCR products were gel-purified and Gibson assembled into StuI-linearized pMTL-YN1C to construct pMTL-YN1C-*hypD* and pMTL-YN1C-*proC*. Gibson assembly reactions were transformed into *E. coli* TOP10 cells and then plated out onto LB-chloramphenicol (25 μg/mL) agar plates. All plasmids were confirmed by Sanger sequencing and then transformed into *E. coli* HB101/pRK24 for conjugation.

Gene deletions in *C. difficile*. Allele-coupled exchange was used to construct clean deletions of *hypD* and *proC* (45). The recipient *C. difficile* strain 630Δ*erm*Δ*pyrE* (a kind gift from Nigel Minton, c/o Marcin Dembek) was grown for 5–6 h in BHIS medium in an anaerobic chamber (Coy, USA). *E. coli*

HB101/pRK24 donor strains carrying the appropriate pMTL-YN3 allelic exchange constructs were grown in LB medium containing ampicillin (50 μg/mL) and chloramphenicol (20 μg/mL) at 37°C, 225 rpm, under aerobic conditions, for 5–6 h. Each *E. coli* strain was pelleted at 600 g for 5 min and transferred into an anaerobic chamber. One milliliter of the *C. difficile* culture was added to each *E. coli* pellet, and 100 μL of the mixture was spotted seven times onto a BHIS plate. The *E. coli* and *C. difficile* mixture was incubated for 13–18 h at 37°C anaerobically, after which the resulting growth was scraped from the plate into 1 mL phosphate-buffered saline (PBS). One hundred microliter aliquots of each suspension were spread onto five BHIS plates containing 10 μg/mL thiamphenicol, 50 μg/mL kanamycin, and 8 μg/mL cefoxitin. The plates were incubated for 3–4 days at 37°C, and transconjugants were passaged onto BHIS plates containing 15 μg/mL thiamphenicol, 50 μg/mL kanamycin, 8 μg/mL cefoxitin, and 5 μg/mL uracil. After selecting for the fastest growing colonies over 2–3 passages, single colonies were restruck onto CDMM plates, a defined minimal medium, containing 2 mg/mL 5-fluoroorotic acid (FOA) and 5 μg/mL uracil. FOA-resistant colonies that arose were patched onto CDMM plates containing 5-FOA and uracil, and colony PCR was performed to identify clones harboring the desired deletions (46)(Table S1). Mutants were further verified by Sanger sequencing PCR products. All 630Δ*erm*Δ*pyrE* mutant strains were complemented with *pyrE* in the *pyrE* locus as described in the next section.

Complementation in *C. difficile*. *E. coli* HB101/pRK24 donor strains carrying the appropriate complementation construct were grown in LB containing ampicillin (50 μg/mL) and chloramphenicol (20 μg/mL) at 37°C, under aerobic conditions, for 6 h (46, 47). For complementation in the *pyrE* locus using pMTL-YN1C constructs, *C. difficile* recipient strains were conjugated with either the empty pMTL-YN1C vector or the appropriate pMTL-YN1C complementation vectors as described previously. Transconjugants were then restruck onto CDMM and incubated for 2–4 days. Colonies that had restored the *pyrE* locus by virtue of their ability to grow on CDMM were restruck onto CDMM plates before further characterization. All clones were verified by colony PCR. At least two independent clones from each complementation strain were phenotypically characterized.

Genomic analysis of *hypD* and *proC*. This was performed using the gggenes package (version 0.4.0) in R (version 3.6.3) and Geneious as described previously (16). Briefly, the *hypD* comparison was constructed by first extracting the positional information for *hypD* and *proC* from Geneious (35), then obtaining amino acid identity percentage through BLASTp alignments (36) against coding sequences from the reference strain *C. scindens* ATCC 35704 (NCBI accession no. PRJNA508260). These data were visualized using the publicly available gggenes R package (37).

RNA extraction. *C. difficile*, *C. scindens*, *C. hiranonis*, and *C. hylemonae* liquid cultures were started from a single colony and grown in either BHI or BHI + 600 mg/L (4.6 mM) hydroxyproline media for 14 h before RNA extraction. Cultures were fixed by adding equal volumes of a 1:1 mixture of EtOH and acetone and stored at −80°C for later RNA extraction. For extraction, the culture was thawed, then centrifuged at 10,000 rpm for 10 min at 4°C. The supernatant was discarded and the cell pellet resuspended in 1 mL of 1:100 BME: (beta-mercaptoethanol)H_2O, then spun down at 14,000 rpm for 1 min. For RNA to be used for qRT-PCR, the cell pellet was resuspended in 0.3 mL of lysis buffer from the Ambion RNA purification kit (AM1912, Invitrogen) then sonicated while on ice for 10 pulses of 2 s with a pause of 3 s between each pulse. Extraction was then performed following the manufacturer's protocol from the Ambion RNA purification kit. For RNA to be used for RNA-seq, the cell pellet was resuspended in 1 mL of TRIzol (Thermofisher F) and incubated at room temperature for 15 min. Two hundred μL of chloroform (Sigma-Aldrich) was added, and the solution was inverted rapidly for 20 s, then incubated at room temperature for 15 min and centrifuged at 14,000 rpm for 15 min at 4°C. The aqueous phase was mixed with 96% ethanol and the extraction was performed using the Direct-zol RNA Miniprep Plus following the manufacturer's instructions, including an on-column DNase I treatment (R2071, Zymo Research).

Reverse transcription and quantitative real-time PCR. Reverse transcription and quantitative real-time PCR (qRT-PCR) was performed as described previously (15). Briefly, RNA was depleted by using Turbo DNase according to the manufacturer's instructions (AM2238, Invitrogen). The DNase-treated RNA was then cleaned using an RNA clean-up kit (R1019, Zymo) according to manufacturer's instructions, and DNA depletion was verified by amplifying 1 μL of RNA in a PCR. The DNA depleted RNA was used as the template for reverse transcription performed with Moloney murine leukemia virus (MMLV) reverse transcriptase (M0253, NEB). The cDNA samples were then diluted 1:4 in water and used in quantitative real-time PCR with gene-specific primers using SsoAdvanced Universal Sybr Green Supermix (1725271, Bio-Rad) according to the manufacturer's protocol (Table S1). Amplifications were performed in technical triplicates, and copy numbers were calculated using a standard curve and normalized to that of a housekeeping gene. *gyrA* was the housekeeping gene used for *C. scindens*, while *rpoC* was used for *C. difficile*, *C. hiranonis*, and *C. hylemonae* (16).

RNAseq. Sequencing of RNA derived from *in vitro* cultures was performed at the Roy J. Carver Biotechnology Center at the University of Illinois at Urbana-Champaign. rRNA was removed from the samples using the RiboZero Epidemiology Kit (Illumina). RNAseq libraries were prepped with the TruSeq Stranded mRNA Sample Prep Kit (Illumina), though poly-A enrichment was omitted. Library quantification was done via qPCR, and the samples were sequenced on one lane for 151 cycles from each end of the fragments on a NovaSeq 6000 using a NovaSeq S4 reagent kit. The FASTQ files were generated and demultiplexed using the bcl2fastq v2.20 Conversion Software (Illumina). Raw paired Illumina reads were imported into Geneious 10.2.6, where adapters were removed using BBDuk with a Kmer length of 27. The reads were mapped to the *C. difficile* 630Δ*erm* genome (NCBI accession no. NC_009089.1), the *C. hiranonis* DSM 13275 genome (NCBI accession no. GCA_008151785.1), the *C. hylemonae* DSM 15053 genome (NCBI accession no. PRJNA523213), or the *C. scindens* ATCC 35704 genome (NCBI accession no. PRJNA508260) using BBMap with a Kmer length of 10 and no other changes to the default settings. Differential expression analysis between the two conditions was performed using DESeq2, and if genes

had an adjusted *P* value of <0.05 and ± 1 $\log_2$ fold change, they were considered differentially expressed. Visualization of differentially enriched genes for each organism was performed using pheatmap (version 1.0.12), ggplots (version 3.3.4), and ggpubr (version 0.4.0.999) within R (version 3.6.3). Some of the differentially enriched genes were hypothetical proteins; those results were removed before the figures were visualized. Full RNAseq data are available in Data File S4.

Metabolomics data analysis. (i) *Mass spectrometry data acquisition.* Samples collected after 14 h of growth were diluted 1:100 (10 μL sample, 990 μL water) and transferred to an autosampler vial for analysis by UPLC-MS. For quantification of amino acids, a certified reference material amino acid mix solution (*Trace*CERT, Sigma) was diluted to achieve a 100 μM working standard solution. Ten calibration standards ranging from 100 μM to 250 nM were prepared by serially diluting the working standard solution. For quantification of 4-hydroxyproline and 5-aminovaleric acid, certified reference material (Sigma) for each was suspended in water to achieve a 1 mg/mL solution, which was combined and diluted to achieve a 50 μg/mL working standard solution. Ten calibration standards ranging from 50 μg/mL to 25 ng/mL were prepared by serially diluting the working standard solution. The analysis was performed using a Thermo Vanquish UPLC instrument (Thermo Fisher Scientific, Germering, Germany) coupled to a Thermo Orbitrap Exploris 480 mass spectrometer (Thermo Fisher Scientific, Breman, Germany) with a heated electrospray ionization (HESI) source. Chromatographic separation was achieved on a Waters BEH Amide column (2.1 $\times$ 100 mm, 1.8 μM) maintained at 45°C. The following linear gradient of mobile phase A (H_2O + 0.1% FA) and mobile phase B (MeCN + 0.1% FA) was used: 0–0.1 min (99% B, 0.4 mL/min), 0.1–7 min (99–30%B, 0.4 mL/min), 7–10 min (99%B, 0.4 mL/min). Samples were analyzed (2 μL injections) in positive ion mode (spray voltage 3.5 kV, ion transfer tube temperature 300°C, vaporizer temperature 350°C, sheath gas 50 a.u. (arbitrary units), auxillary gas 10 a.u., sweep gas 1 a.u.) with a mass range of *m/z* 60–1000. MS1 data was collected with a resolving power of 60,000 and an AGC target of 1e6, and ddMS2 data were collected with a resolving power of 30,000, cycle time of 0.6 s, AGC target of 4e5, and stepped HCD collision energy (30, 50, 150). The full data set was acquired in a randomized fashion with water blanks and system suitability samples (QReSS, Cambridge Isotope Laboratories) collected every 10 samples.

(ii) Targeted data processing. Peak integration and amino acid quantification were performed in Skyline[1]. Individual standard curves for each of the 15 amino acids plus hydroxyproline and 5-aminovalerate were constructed using extracted ion chromatogram peak areas from MS1 data, and the slope of each curve was calculated using a linear curve fit and a 1/(x *x) weighting. MS2 data were utilized to validate amino acid annotations, particularly to differentiate valine and 5-aminovaleric acid. The concentrations in the study samples were calculated in an identical manner relative to the regression line. Calibration curves for each of the amino acids had R^2 values ranging from 0.9919 to 0.9994 for the linear range of 0.25 to 100 μM. Calibration curves for 4-hydroxyproline and 5-aminovaleric acid had R^2 values of 0.9948 to 0.9997, respectively, for the linear range of 0.025 to 50 μg/mL (48).

16S rRNA bacterial sequencing. Fecal and cecal samples were sequenced by the University of Michigan Microbial Systems Molecular Biology Laboratory using the Illumina MiSeq platform (49). Microbial DNA was extracted from the fecal and cecal samples using the Mag Attract Power Microbiome kit (Mo Bio Laboratories, Inc.). A dual-indexing sequencing strategy was used to amplify the V4 region of the 16S rRNA gene. Each 20-μL PCR mixture contained 2 μL of 10$\times$ Accuprime PCR buffer II (Life Technologies, CA, USA), 0.15 μL of Accuprime high-fidelity polymerase (Life Technologies, CA, USA), 5 μL of a 4.0 μM primer set, 3 μL DNA, and 11.85 μL sterile nuclease free water. The template DNA concentration was 1 to 10 ng/μL for a high bacterial DNA/host DNA ratio. The PCR conditions were as follows: 2 min at 95°C, followed by 30 cycles of 95°C for 20 s, 55°C for 15 s, and 72°C for 5 min, followed by 72°C for 10 min. Libraries were normalized using a Life Technologies SequalPrep normalization plate kit as per manufacturer's instructions for sequential elution. The concentration of the pooled samples was determined using the Kapa Biosystems library quantification kit for Illumina platforms (Kapa Biosystems, MA, USA). Agilent Bioanalyzer high sensitivity DNA analysis kit (Agilent CA, USA) was used to determine the sizes of the amplicons in the library. The final library consisted of equal molar amounts from each of the plates, normalized to the pooled plate at the lowest concentration. Sequencing was done on the Illumina MiSeq platform, using a MiSeq reagent kit V2 (Ilumina, CA, USA) with 500 cycles according to the manufacturer's instructions, with modifications. Sequencing libraries were prepared according to Illumina's protocol for preparing libraries for sequencing on the MiSeq (Ilumina, CA, USA) for 2 or 4 nM libraries. PhiX and genomes were added in 16S amplicon sequencing to add diversity. Sequencing reagents were prepared according to the Schloss SOP (https://www.mothur.org/wiki/MiSeq_SOP#Getting_started), and custom read 1, read 2, and index primers were added to the reagent cartridge (49). FASTQ files were generated for paired end reads.

Community microbial sequencing analysis. Analysis of the V4 region of the 16S rRNA gene was performed in the statistical programming environment R using the DADA2 package (version 1.14.1) (50). Forward/reverse pairs were trimmed and filtered, with forward reads truncated at 240 nucleotides (nt) and reverse reads truncated at 200 nt. No ambiguous bases were allowed, and each read was required to have less than two expected errors based on their quality score. Error-corrected amplicon sequence variants (ASVs) were independently inferred for the forward and reverse reads of each sample, and then read pairs were merged to obtain final ASVs. Chimeric ASVs were identified and removed. For taxonomic assignments, ASVs were compared to the Silva v132 database (https://zenodo.org/record/1172783). The R package phyloseq (version 1.30) was used to further analyze and visualize data (38). Inverse Simpson was used to calculate alpha diversity, and Kruskal Wallis was used to determine statistical significance between treatment groups. Relative abundance was calculated using phyloseq and visualized using Prism 7.0c, and differential-abundance analysis between the Δ*hypD* and WT treatment groups was performed using the Aldex2 package (version 1.18.0) and visualized using the ggplots2 package (version 3.3.4) (34, 51, 52).

Statistical analysis. Statistical tests were performed using Prism version 7.0c for Mac OSX (GraphPad Software, La Jolla, CA, USA). Statistical significance was determined using Mann-Whitney for CFU, spore count, and

toxin activity, and Kruskal Wallis with Dunn's multiple comparisons for mouse weights during infection. Student's *t* tests with Welch's correction were applied to account for multiple comparisons in analyses of other data. Statistical analysis for the 16S and RNAseq results was performed in the R computing environment. Kruskal Wallis was used for alpha diversity, Permanova Adonis in the vegan package (version 2.5–7) was used to test the difference between groups for the beta diversity analysis, and ALDEx2 was used to calculate the differences between treatments using a centered-log-ratio transform of ASV abundance to create an effect size for each ASV (34).

Data availability. Raw sequences have been deposited in the Sequence Read Archive (SRA). They can both be found under BioProject ID PRJNA776739. Source data are provided within each supplementary data file. Other data and biological materials are available from the corresponding author upon reasonable requests.

SUPPLEMENTAL MATERIAL

Supplemental material is available online only.

DATA SET S1, XLSX file, 2.7 MB.

DATA SET S2, XLSX file, 0.01 MB.

DATA SET S3, XLSX file, 0.04 MB.

DATA SET S4, XLSX file, 1.9 MB.

FIG S1, PDF file, 0.1 MB.

FIG S2, PDF file, 0.6 MB.

FIG S3, PDF file, 0.1 MB.

FIG S4, PDF file, 0.6 MB.

TABLE S1, DOCX file, 0.02 MB.

ACKNOWLEDGMENTS

We thank Jason Ridlon for providing the commensal *Clostridia* strains. Y.Y.H., D.J.K., and E.P.B. were funded by Faculty Scholar Award and the Packard Fellowship for Science and Engineering from the David and Lucile Packard Foundation (2013-39267). C.M.T. was funded by the National Institute of General Medical Sciences of the National Institutes of Health under award number R35GM119438. This work was performed in part by the Molecular Education, Technology and Research Innovation Center (METRIC) at NC State University, which is supported by the State of North Carolina.

REFERENCES

1. Lessa FC, Mu Y, Bamberg WM, Beldavs ZG, Dumyati GK, Dunn JR, Farley MM, Holzbauer SM, Meek JI, Phipps EC, Wilson LE, Winston LG, Cohen JA, Limbago BM, Fridkin SK, Gerding DN, McDonald LC. 2015. Burden of *Clostridium difficile* infection in the United States. N Engl J Med 372:825–834. https://doi.org/10.1056/NEJMoa1408913.
2. Magill SS, O'Leary E, Janelle SJ, Thompson DL, Dumyati G, Nadle J, Wilson LE, Kainer MA, Lynfield R, Greissman S, Ray SM, Beldavs Z, Gross C, Bamberg W, Sievers M, Concannon C, Buhr N, Warnke L, Maloney M, Ocampo V, Brooks J, Oyewumi T, Sharmin S, Richards K, Rainbow J, Samper M, Hancock EB, Leaptrot D, Scalise E, Badrun F, Phelps R, Edwards JR. 2018. Changes in prevalence of health care-associated infections in U.S. N Engl J Med 379:1732–1744. https://doi.org/10.1056/NEJMoa1801550.
3. Kelly CP. 2012. Current strategies for management of initial *Clostridium difficile* infection. J Hosp Med 7(Suppl 3):S5–S10. https://doi.org/10.1002/jhm.1909.
4. Cornely OA, Miller MA, Louie TJ, Crook DW, Gorbach SL. 2012. Treatment of first recurrence of *Clostridium difficile* infection: fidaxomicin versus vancomycin. Clin Infect Dis 55(Suppl 2):S154–S161. https://doi.org/10.1093/cid/cis462.
5. Fekety R, McFarland LV, Surawicz CM, Greenberg RN, Elmer GW, Mulligan ME. 1997. Recurrent *Clostridium difficile* diarrhea: characteristics of and risk factors for patients enrolled in a prospective, randomized, double-blinded trial. Clin Infect Dis 24:324–333. https://doi.org/10.1093/clinids/24.3.324.
6. Owens RC, Jr, Donskey CJ, Gaynes RP, Loo VG, Muto CA. 2008. Antimicrobial-associated risk factors for *Clostridium difficile* infection. Clin Infect Dis 46(Suppl 1):S19–S31. https://doi.org/10.1086/521859.
7. Seekatz AM, Young VB. 2014. *Clostridium difficile* and the microbiota. J Clin Invest 124:4182–4189. https://doi.org/10.1172/JCI72336.
8. Theriot CM, Koenigsknecht MJ, Carlson PE, Jr, Hatton GE, Nelson AM, Li B, Huffnagle GB, J ZL, Young VB. 2014. Antibiotic-induced shifts in the mouse gut microbiome and metabolome increase susceptibility to *Clostridium difficile* infection. Nat Commun 5:3114. https://doi.org/10.1038/ncomms4114.
9. Ducarmon QR, Zwittink RD, Hornung BVH, van Schaik W, Young VB, Kuijper EJ. 2019. Gut microbiota and colonization resistance against bacterial enteric infection. Microbiol Mol Biol Rev 83:e00007-19. https://doi.org/10.1128/MMBR.00007-19.
10. Crobach MJT, Vernon JJ, Loo VG, Kong LY, Pechine S, Wilcox MH, Kuijper EJ. 2018. Understanding *Clostridium difficile* colonization. Clin Microbiol Rev 31:e00021-17. https://doi.org/10.1128/CMR.00021-17.
11. Buffie CG, Pamer EG. 2013. Microbiota-mediated colonization resistance against intestinal pathogens. Nat Rev Immunol 13:790–801. https://doi.org/10.1038/nri3535.
12. Guo C-J, Allen BM, Hiam KJ, Dodd D, Van Treuren W, Higginbottom S, Nagashima K, Fischer CR, Sonnenburg JL, Spitzer MH, Fischbach MA. 2019. Depletion of microbiome-derived molecules in the host using Clostridium genetics. Science 366:eaav1282. https://doi.org/10.1126/science.aav1282.
13. Battaglioli EJ, Hale VL, Chen J, Jeraldo P, Ruiz-Mojica C, Schmidt BA, Rekdal VM, Till LM, Huq L, Smits SA, Moor WJ, Jones-Hall Y, Smyrk T, Khanna S, Pardi DS, Grover M, Patel R, Chia N, Nelson H, Sonnenburg JL, Farrugia G, Kashyap PC. 2018. *Clostridioides difficile* uses amino acids associated with gut microbial dysbiosis in a subset of patients with diarrhea. Sci Transl Med 10:eaam7019. https://doi.org/10.1126/scitranslmed.aam7019.
14. Fletcher JR, Pike CM, Parsons RJ, Rivera AJ, Foley MH, McLaren MR, Montgomery SA, Theriot CM. 2021. *Clostridioides difficile* exploits toxin-mediated inflammation to alter the host nutritional landscape and exclude competitors from the gut microbiota. Nat Commun 12:462. https://doi.org/10.1038/s41467-020-20746-4.
15. Fletcher JR, Erwin S, Lanzas C, Theriot CM. 2018. Shifts in the gut metabolome and *Clostridium difficile* transcriptome throughout colonization and infection in a mouse model. mSphere 3:e00089-18. https://doi.org/10.1128/mSphere.00089-18.

16. Reed AD, Nethery MA, Stewart A, Barrangou R, Theriot CM. 2020. Strain-dependent inhibition of *Clostridioides difficile* by commensal *Clostridia* encoding the bile acid inducible (*bai*) operon. J Bacteriol 202:e00039-20. https://doi.org/10.1128/JB.00039-20.
17. Winston JA, Rivera AJ, Cai J, Thanissery R, Montgomery SA, Patterson AD, Theriot CM. 2020. Ursodeoxycholic acid (UDCA) mitigates the host inflammatory response during *Clostridioides difficile* infection by altering gut bile acids. Infect Immun 88:e00045-20. https://doi.org/10.1128/IAI.00045-20.
18. Ridlon JM, Harris SC, Bhowmik S, Kang DJ, Hylemon PB. 2016. Consequences of bile salt biotransformations by intestinal bacteria. Gut Microbes 7:22–39. https://doi.org/10.1080/19490976.2015.1127483.
19. Buffie CG, Bucci V, Stein RR, McKenney PT, Ling L, Gobourne A, No D, Liu H, Kinnebrew M, Viale A, Littmann E, van den Brink MRM, Jenq RR, Taur Y, Sander C, Cross JR, Toussaint NC, Xavier JB, Pamer EG. 2015. Precision microbiome reconstitution restores bile acid mediated resistance to *Clostridium difficile*. Nature 517:205–208. https://doi.org/10.1038/nature13828.
20. Sorg JA, Sonenshein AL. 2010. Inhibiting the initiation of *Clostridium difficile* spore germination using analogs of chenodeoxycholic acid, a bile acid. J Bacteriol 192:4983–4990. https://doi.org/10.1128/JB.00610-10.
21. Wilson KH, Sheagren JN. 1983. Antagonism of toxigenic *Clostridium difficile* by nontoxigenic *C. difficile*. J Infect Dis 147:733–736. https://doi.org/10.1093/infdis/147.4.733.
22. Gerding DN, Meyer T, Lee C, Cohen SH, Murthy UK, Poirier A, Van Schooneveld TC, Pardi DS, Ramos A, Barron MA, Chen H, Villano S. 2015. Administration of spores of nontoxigenic *Clostridium difficile* strain M3 for prevention of recurrent *C. difficile* infection: a randomized clinical trial. JAMA 313:1719–1727. https://doi.org/10.1001/jama.2015.3725.
23. Jenior ML, Leslie JL, Powers DA, Garrett EM, Walker KA, Dickenson ME, Petri WA, Tamayo R, Papin JA. 2021. Novel drivers of virulence in *Clostridioides difficile* identified via context-specific metabolic network analysis. bioRxiv https://doi.org/10.1101/2020.11.09.373480.
24. Jenior ML, Leslie JL, Young VB, Schloss PD. 2017. *Clostridium difficile* colonizes alternative nutrient niches during infection across distinct murine gut microbiomes. mSystems 2:e00063-17. https://doi.org/10.1128/mSystems.00063-17.
25. Lovitt RW, Kell DB, Morris JG. 1986. Proline reduction by *Clostridium sporogenes* is coupled to vectorial proton ejection. FEMS Microbiology Lett 36:269–273. https://doi.org/10.1111/j.1574-6968.1986.tb01708.x.
26. Liu Y, Chen H, Treuren WV, Hou BH, Higginbottom SK, Sonnenburg JL, Dodd D. 2021. Electron transfer proteins in gut bacteria yield metabolites that circulate in the host. bioRxiv https://doi.org/10.1101/2019.12.11.873224.
27. Bouillaut L, Self WT, Sonenshein AL. 2013. Proline-dependent regulation of *Clostridium difficile* Stickland metabolism. J Bacteriol 195:844–854. https://doi.org/10.1128/JB.01492-12.
28. Karasawa T, Ikoma S, Yamakawa K, Nakamura S. 1995. A defined growth medium for *Clostridium difficile*. Microbiology 141:371–375. https://doi.org/10.1099/13500872-141-2-371.
29. Gencic S, Grahame DA. 2020. Diverse energy-conserving pathways in *Clostridium difficile*: growth in the absence of amino acid Stickland acceptors and the role of the Wood-Ljungdahl pathway. J Bacteriol 202:e00233-20. https://doi.org/10.1128/JB.00233-20.
30. Gorres KL, Raines RT. 2010. Prolyl 4-hydroxylase. Crit Rev Biochem Mol Biol 45:106–124. https://doi.org/10.3109/10409231003627991.
31. Huang YY, Martinez-Del Campo A, Balskus EP. 2018. Anaerobic 4-hydroxyproline utilization: discovery of a new glycyl radical enzyme in the human gut microbiome uncovers a widespread microbial metabolic activity. Gut Microbes 9:437–451. https://doi.org/10.1080/19490976.2018.1435244.
32. Levin BJ, Huang YY, Peck SC, Wei Y, Martinez-Del Campo A, Marks JA, Franzosa EA, Huttenhower C, Balskus EP. 2017. A prominent glycyl radical enzyme in human gut microbiomes metabolizes trans-4-hydroxy-l-proline. Science 355:eaai8386. https://doi.org/10.1126/science.aai8386.
33. Lopez CA, McNeely TP, Nurmakova K, Beavers WN, Skaar EP. 2020. *Clostridioides difficile* proline fermentation in response to commensal clostridia. Anaerobe 63:102210. https://doi.org/10.1016/j.anaerobe.2020.102210.
34. Gloor G. 2015. ALDEx2: ANOVA-Like Differential Expression tool for compositional data. ALDEX Manual Modular 20:1–11.
35. Neumann-Schaal M, Jahn D, Schmidt-Hohagen K. 2019. Metabolism the difficile way: the key to the success of the pathogen *Clostridioides difficile*. Front Microbiol 10:219. https://doi.org/10.3389/fmicb.2019.00219.
36. Hensbergen PJ, Klychnikov OI, Bakker D, Dragan I, Kelly ML, Minton NP, Corver J, Kuijper EJ, Drijfhout JW, van Leeuwen HC. 2015. *Clostridium difficile* secreted Pro-Pro endopeptidase PPEP-1 (ZMP1/CD2830) modulates adhesion through cleavage of the collagen binding protein CD2831. FEBS Lett 589:3952–3958. https://doi.org/10.1016/j.febslet.2015.10.027.
37. Udenfriend S. 1966. Formation of hydroxyproline in collagen. Science 152:1335–1340. https://doi.org/10.1126/science.152.3727.1335.
38. Winston JA, Thanissery R, Montgomery SA, Theriot CM. 2016. Cefoperazone-treated mouse model of clinically-relevant *Clostridium difficile* strain R20291. J Vis Exp 118:e54850.
39. Koenigsknecht MJ, Theriot CM, Bergin IL, Schumacher CA, Schloss PD, Young VB. 2015. Dynamics and establishment of *Clostridium difficile* infection in the murine gastrointestinal tract. Infect Immun 83:934–941. https://doi.org/10.1128/IAI.02768-14.
40. Theriot CM, Koumpouras CC, Carlson PE, Bergin II, Aronoff DM, Young VB. 2011. Cefoperazone-treated mice as an experimental platform to assess differential virulence of *Clostridium difficile* strains. Gut Microbes 2:326–334. https://doi.org/10.4161/gmic.19142.
41. Ridlon JM, Devendran S, Alves JM, Doden H, Wolf PG, Pereira GV, Ly L, Volland A, Takei H, Nittono H, Murai T, Kurosawa T, Chlipala GE, Green SJ, Hernandez AG, Fields CJ, Wright CL, Kakiyama G, Cann I, Kashyap P, McCracken V, Gaskins HR. 2020. The "*in vivo* lifestyle" of bile acid 7alpha-dehydroxylating bacteria: comparative genomics, metatranscriptomic, and bile acid metabolomics analysis of a defined microbial community in gnotobiotic mice. Gut Microbes 11:381–404. https://doi.org/10.1080/19490976.2019.1618173.
42. Aguirre AM, Yalcinkaya N, Wu Q, Swennes A, Tessier ME, Roberts P, Miyajima F, Savidge T, Sorg JA. 2021. Bile acid-independent protection against *Clostridioides difficile* infection. PLoS Pathog 17:e1010015. https://doi.org/10.1371/journal.ppat.1010015.
43. Thanissery R, Winston JA, Theriot CM. 2017. Inhibition of spore germination, growth, and toxin activity of clinically relevant *C. difficile* strains by gut microbiota derived secondary bile acids. Anaerobe 45:86–100. https://doi.org/10.1016/j.anaerobe.2017.03.004.
44. Thanissery R, Zeng D, Doyle RG, Theriot CM. 2018. A small molecule-screening pipeline to evaluate the therapeutic potential of 2-aminoimidazole molecules against *Clostridium difficile*. Front Microbiol 9:1206. https://doi.org/10.3389/fmicb.2018.01206.
45. Gibson DG, Young L, Chuang RY, Venter JC, Hutchison CA, 3rd, Smith HO. 2009. Enzymatic assembly of DNA molecules up to several hundred kilobases. Nat Methods 6:343–345. https://doi.org/10.1038/nmeth.1318.
46. Fimlaid KA, Jensen O, Donnelly ML, Francis MB, Sorg JA, Shen A. 2015. Identification of a novel lipoprotein regulator of *Clostridium difficile* spore germination. PLoS Pathog 11:e1005239. https://doi.org/10.1371/journal.ppat.1005239.
47. Putnam EE, Nock AM, Lawley TD, Shen A. 2013. SpoIVA and SipL are *Clostridium difficile* spore morphogenetic proteins. J Bacteriol 195:1214–1225. https://doi.org/10.1128/JB.02181-12.
48. Adams KJ, Pratt B, Bose N, Dubois LG, St John-Williams L, Perrott KM, Ky K, Kapahi P, Sharma V, MacCoss MJ, Moseley MA, Colton CA, MacLean BX, Schilling B, Thompson JW, Alzheimer's Disease Metabolomics Consortium. 2020. Skyline for small molecules: a unifying software package for quantitative metabolomics. J Proteome Res 19:1447–1458. https://doi.org/10.1021/acs.jproteome.9b00640.
49. Kozich JJ, Westcott SL, Baxter NT, Highlander SK, Schloss PD. 2013. Development of a dual index sequencing strategy and curation pipeline for analyzing amplicon sequence data on the MiSeq Illumina sequencing platform. Appl Environ Microbiol 79:5112–5120. https://doi.org/10.1128/AEM.01043-13.
50. Callahan BJ, McMurdie PJ, Rosen MJ, Han AW, Johnson AJA, Holmes SP. 2016. DADA2: high-resolution sample inference from Illumina amplicon data. Nat Methods 13:581–583. https://doi.org/10.1038/nmeth.3869.
51. Gómez-Rubio V. 2017. ggplot2-elegant graphics for data analysis. J Stat Soft 77:1–3. https://doi.org/10.18637/jss.v077.b02.
52. McMurdie PJ, Holmes S. 2013. phyloseq: an R package for reproducible interactive analysis and graphics of microbiome census data. PLoS One 8:e61217. https://doi.org/10.1371/journal.pone.0061217.